

# THERMAL INSTABILITY AND THE FORMATION OF CLUMPY GAS CLOUDS

A. Burkert<sup>1</sup> and D. N. C. Lin<sup>2</sup>

Received \_\_\_\_\_; accepted \_\_\_\_\_

*Astrophysical Journal, in press*

---

<sup>1</sup>Max-Planck-Institut für Astronomie, Königstuhl 17, D-69117 Heidelberg, Germany. E-mail:  
burkert@mpia-hd.mpg.de

<sup>2</sup>UCO/Lick Observatory, University of California, Santa Cruz, California, 95064. E-mail:  
lin@lick.ucolick.org

## ABSTRACT

The radiative cooling of optically thin gaseous regions and the formation of a two-phase medium and of cold gas clouds with a clumpy substructure is investigated. We demonstrate how clumpiness can emerge as a result of thermal instability. In optically thin clouds, the growth rate of small density perturbations is independent of their length scale as long as the perturbations can adjust to an isobaric state. However, the growth of a perturbation is limited by its transition from isobaric to isochoric cooling when the cooling time scale is reduced below the sound crossing time scale across its length scale. The temperature at which this transition occurs decreases with the length scale of the perturbation. Consequently small scale perturbations have the potential to reach higher amplitudes than large scale perturbations. When the amplitude becomes nonlinear, advection overtakes the pressure gradient in promoting the compression resulting in an accelerated growth of the disturbance. The critical temperature for transition depends on the initial amplitude. The fluctuations which can first reach nonlinearity before their isobaric to isochoric transition will determine the characteristic size and mass of the cold dense clumps which would emerge from the cooling of an initially nearly homogeneous region of gas. Thermal conduction is in general very efficient in erasing isobaric, small-scale fluctuations, suppressing a cooling instability. A weak, tangled magnetic field can however reduce the conductive heat flux enough for low-amplitude fluctuations to grow isobarically and become non-linear if their length scales are of order  $10^{-2}$  pc. If the amplitude of the initial perturbations is a decreasing function of the wavelength, the size of the emerging clumps will decrease with increasing magnetic field strength. Finally, we demonstrate how a 2-phase medium, with cold clumps being pressure confined in a diffuse hot residual background component, would be sustained if there is adequate heating to compensate the energy loss.

*Subject headings:* globular clusters: general — instabilities — ISM: clouds, formation

## 1. Introduction

The interstellar medium and cold gas clouds are characterized by a clumpy substructure and a turbulent velocity field (Larson 1981, Blitz 1993). As molecular clouds are the sites of star formation, their formation, internal structure and dynamics determines the rate of star formation and the properties of young stars, such as their mass function or binarity. The understanding of the origin of cold clouds and their internal substructure is therefore of fundamental importance for a consistent theory of star formation and galactic evolution.

In the nearby clouds, the dispersion velocity inferred from molecular line width is often larger than the gas sound speed inferred from the line transition temperatures (Solomon et al 1987). MHD turbulence may be responsible for the stirring of these clouds (Arons & Max 1975). This conjecture is supported by the polarization maps and direct measurements of field strength in some star forming regions (Myers & Goodman 1988, Crutcher et al. 1993). Recent simulations of MHD turbulence, however, suggest that it dissipates rapidly (Gammie & Ostriker 1996, MacLow et al 1998, MacLow 1999, Ostriker et al. 1999). One possible source of energy supply is winds and outflows from young stellar objects (Franco & Cox 1983, McKee 1989). But in regions where star formation is inactive, clumpy structure with velocity dispersion is also observed. Thus, the origin and energy supply of clumpy cloud structure remains an outstanding issue.

On small scales, magnetic field pressure is important in regulating infall and collapse of protostellar clouds and the formation of low-mass stars (Mouschovias & Spitzer 1976, Nakano 1979, Shu 1993). For clouds with sub-critical masses, gravitational contraction is preceded by ambipolar diffusion which for typical cloud densities operates on a timescale  $\tau_B \sim 10^{7-8}$  yr (Lizano & Shu 1989, Mouschovias 1991). In regions with intense star formation activities such as the central region of Orion,  $\tau_B$  for individual dense clumps is comparable to the typical age of the young stellar objects. But, the spread in stellar ages ( $\Delta\tau_* \sim 10^6$  yrs) appears to be considerably shorter than  $\tau_B$  (Carpenter et al. 1997, Hillenbrand, 1997). This coeval star formation history requires either a coordinated trigger mechanism for star formation within initially magnetically supported clumps or subcritical collapse, fragmentation and star formation of a larger molecular cloud region in which the magnetic field plays a weak role.

A rapid and coordinated episode of star formation can also be inferred in globular clusters (Brown et al. 1991, 1995, Murray & Lin 1992, Lin & Murray 1992). In some metal deficient clusters such as M92, the total amount of heavy elements corresponds to the yield of a few supernovae. If star formation has proceeded over a duration  $\Delta\tau_*$  comparable to the expected life span ( $\sim$  a few  $10^6$  yrs) of massive stars,

a significant metallicity spread would be expected, in contrast to the observations (e.g. Kraft 1979). At least in these systems,  $\Delta\tau_* < \tau_B$  and star formation may have proceeded through supercritical collapse. The dynamical timescale of most clusters at their half mass radius is  $\tau_d \approx 10^6$  yr. Any energy dissipation associated with the episode of star formation would imply an even longer dynamical timescale in the proto cluster cloud prior to that event. We infer that  $\Delta\tau_*$  was comparable to or shorter than the dynamical timescale of the proto cluster clouds indicating a rapid fragmentation and star formation episode.

In this paper, we focus on the rapid emergence of clumpy structure during the formation and collapse of a thermally unstable supercritical cloud. This process is relevant to the formation of stellar clusters as well as galaxies. We assume that the clouds condense out of a diffuse hot medium as a result of thermal instability. Large condensations with cooling timescales  $\tau_c > \tau_d$  are thermally stable because they can adjust through contraction such that their radiative losses may be compensated by the release of their gravitational energy. Runaway cooling of the gas through thermal instability however occurs in clouds with  $\tau_c < \tau_d$ . In order to form clumps within an initially almost homogeneous cloud, internal density fluctuations must grow rapidly on a timescale short compared to the mean dynamical timescale of the entire cloud. Small scale density fluctuations would begin to dominate if either the growth timescale or the limiting amplitude is a decreasing function of the perturbations' length scale. One possible fragmentation mechanism is gravitational collapse. The reduction in the cloud's temperature reduces its Jeans' mass, leading to the onset of gravitational instability and collapse. However, for a non rotating, cold, homogeneous gaseous region, gravitational instability alone cannot induce fragmentation because the growth rate is essentially independent of length scale such that the growth timescale for the density contrast is comparable to the dynamical timescale of the whole cloud (Hunter 1962). This has also been shown by numerical collapse simulations of initially gravitationally unstable perturbed gas clouds (e.g. Burkert & Bodenheimer 1993, 1996, Burkert, Bate & Bodenheimer 1997). If the initial density perturbations  $\delta_0$  are linear ( $\delta_0 < 1$ ), fragmentation is suppressed until the gas cloud has collapsed into either a disk or a dense filamentary substructure.

We propose that clumpyness in clouds arises naturally from their formation through a cooling instability which acts on timescales that can be much shorter than the dynamical timescale of the cloud. In a pioneering paper, Field (1965) derived a criterion for a cooling gas to be unstable to the growth of thermal condensations. He showed that thermal instability can lead to the rapid growth of density perturbations from infinitesimal  $\delta_0$  to nonlinear amplitudes on a cooling timescale  $\tau_c$  which for typical conditions in the interstellar medium is short compared to the dynamical timescale. If  $\tau_c$  increases with decreasing density

any small density difference would induce a temperature difference between the cooler perturbed region and the warmer background. Across the interface between the two-phase medium, differential cooling leads to a pressure gradient which induces a gas flow from the lower-density background towards the higher-density perturbed region. The density enhancement in the cooler region further reduces its cooling timescale compared to that of the background where  $\tau_c$  increases. A more detailed investigation of the growth of condensations in cooling regions has been presented by Schwarz et al. (1972) who included also the effects of ionization and recombination and by Balbus (1986) who examined the effect of magnetic fields. The classical model of the interstellar medium where heating balances cooling was presented by Field et al. (1969). A recent progress report on the theory of thermal instability is given by Balbus (1995).

Although thermal instability proceeds faster than the collapse of the cloud, its growth rate is determined by the local cooling rate. During the initial linear evolution, variations in the initial over density (or under temperature) might lead only to a weak dependence of the growth timescale on the wavelength. In this paper we show however that there exist two important transitions which are very sensitively determined by the wavelengths of perturbations. 1) The growth of a perturbation is limited by its transition from isobaric to isochoric cooling, when the cooling time scale is reduced below the sound crossing time scale across the wavelength of the perturbation. This transition occurs at a lower temperature, with correspondingly larger over density, for perturbations with smaller wavelengths. 2) For those perturbation which can become nonlinear before the isobaric to isochoric transition, advection overtakes the pressure gradient in promoting the compression and growth of the perturbed region at an accelerated rate. The fluctuations which can first reach nonlinearity would dominate the growth of all perturbations with longer wavelengths and homogenize disturbances with smaller wavelengths. Thus, they determine the characteristic size and mass of the cold dense clumps which would emerge from the cooling of an initially nearly homogeneous cloud. Thermal conduction could in general erase these fluctuations, suppressing the instability. Weak, tangled magnetic fields would however be efficient enough in reducing the conductive flux, allowing the medium to break up into cold clumps on the characteristic length scale.

We study the cooling and fragmentation of gas using simplified power-law cooling functions. Since we are primarily interested in supercritical clouds, we neglect the effect of magnetic fields. Note that even a weak magnetic field could have an important destabilizing influence in thermal instability (Loewenstein 1990, Balbus 1995). In §2, we obtain approximate analytic solutions which describe the evolution of a linear density perturbation in the isobaric and nearly isochoric regime. We show that the growth of over density in a thermally unstable fluctuation is limited by a transition from isobaric to isochoric evolution and that

the limiting amplitude is a decreasing function of the length scale. We verify our analytic approximations with numerical, hydrodynamical calculations which are also used in §3 to study the transition into the non-linear regime. In §4 we investigate the cooling of interacting perturbations and determine the critical length scale of clumps that emerge through thermal instability. The importance of thermal conduction is investigated in §5. In §6 we discuss the affect of heating processes and the formation of a stable 2-phase medium. Finally, we summarize our results and discuss their implications in §7.

## 2. The Initial Evolution of Thermal Instability

The dynamical evolution of the gas is described by the hydrodynamical equations

$$\frac{\partial \rho}{\partial t} + \sum_{k=1}^3 \frac{\partial \rho U_k}{\partial x_k} = 0 \quad (1)$$

$$\frac{\partial U_j}{\partial t} + \sum_{k=1}^3 U_k \frac{\partial U_j}{\partial x_k} + \frac{R_g}{\mu \rho} \frac{\partial}{\partial x_j} (\rho T) = 0 \quad (2)$$

$$\frac{\partial T}{\partial t} + \sum_{k=1}^3 U_k \frac{\partial T}{\partial x_k} + (\Gamma - 1) T \sum_{k=1}^3 \frac{\partial U_k}{\partial x_k} = -\frac{\rho \Lambda}{C_v} \quad (3)$$

where  $j=1,2,3$  is the coordinate index,  $C_v = R_g/\mu(\Gamma - 1)$  is the heat capacity,  $R_g, \mu$  and  $\Gamma$  are the gas constant, mean molecular weight and adiabatic index, respectively.

In the unperturbed state, the gas remains at rest ( $U_j = 0$ ) and its density attains a constant value,  $\rho_0$ . The time dependent energy equation (3) gives

$$C_v \frac{\partial T_0}{\partial t} = -\rho_0 \Lambda \quad (4)$$

where the cooling rate  $\Lambda = \Lambda_0 T_0^\beta$ . The power index is determined by the detailed atomic processes. Since we are primarily interested in the physical evolution of thermal instability, we adopt a simple constant  $\beta$  prescription. The cooling would be thermally unstable (with  $\tau_c = T_0/\partial T_0/\partial t$  as an increasing function of  $T_0$ ) in the isochoric region if  $\beta < 1$  and in the isobaric region if  $\beta < 2$ . In the absence of external heating, the unperturbed gas temperature  $T_0$  can be expressed as a function of the dimensionless time variable  $\tau \equiv t/\tau_c(0)$  such that

$$T_0(t) = T_0(0) (1 - (1 - \beta)\tau)^{\frac{1}{1-\beta}} \quad (5)$$

where  $T_0(0)$  and  $\tau_c(0) \equiv C_v/\rho_0 \Lambda_0 T_0(0)^{\beta-1}$  are the initial (at  $t = 0$ ) temperature and cooling timescale, respectively.

## 2.1. The Perturbed Quantities

The evolution of the perturbed density ( $\rho_1 = \rho - \rho_0$ ), temperature ( $T_1 = T - T_0$ ), and velocities ( $U_j$ ) are derived from the linearization of the equations (1) to (3):

$$\frac{\partial \rho_1}{\partial t \rho_0} = - \sum_{j=1}^3 \frac{\partial U_j}{\partial x_j}, \quad (6)$$

$$\frac{\partial U_j}{\partial t} = - \frac{R_g T_0}{\mu} \frac{\partial}{\partial x_j} \left( \frac{T_1}{T_0} + \frac{\rho_1}{\rho_0} \right), \quad (7)$$

and

$$\frac{\partial T_1}{\partial t T_0} = -(\Gamma - 1) \sum_{j=1}^3 \frac{\partial U_j}{\partial x_j} - \frac{1}{\tau_c} \left( \frac{\rho_1}{\rho_0} + (\beta - 1) \frac{T_1}{T_0} \right) \quad (8)$$

where

$$\tau_c(t) \equiv - \frac{T_0}{dT_0/dt} = \tau_c(0) - (1 - \beta)t$$

is the characteristic cooling timescale at the instant of time  $t$ .

Since the perturbation equations are linear in  $x_j$ , we adopt a local approximation in which the positional dependence of all the perturbed quantities is proportional to  $\exp(ik_j x_j)$  where  $k_j$  is the wave number in the  $j$ th direction. Substituting a dimensionless velocity variable  $V_j = ik_j \tau_c(0) U_j$ , the perturbed equations reduce to

$$\frac{\partial \rho_1}{\partial \tau \rho_0} = - \sum_{j=1}^3 V_j, \quad (9)$$

$$\frac{\partial V_j}{\partial \tau} = K_j^2 (1 - (1 - \beta)\tau)^{\frac{1}{1-\beta}} \left( \frac{P_1}{P_0} \right), \quad (10)$$

where  $\frac{P_1}{P_0} = \frac{T_1}{T_0} + \frac{\rho_1}{\rho_0}$  is the perturbed pressure,  $K_j \equiv \tau_c(0) k_j \sqrt{R_g T_0(0)/\mu}$  is the ratio of the initial cooling to sound crossing timescale over a characteristic wavelength  $2\pi/k_j$ , and

$$\frac{\partial T_1}{\partial \tau T_0} = -(\Gamma - 1) \sum_{j=1}^3 V_j - \frac{\tau_c(0)}{\tau_c} \left( \frac{\rho_1}{\rho_0} + (\beta - 1) \frac{T_1}{T_0} \right). \quad (11)$$

For a perfect gas, the unperturbed pressure  $P_0 = R_g \rho_0 T_0 / \mu$  decreases at the same rate everywhere. We find from Eqs (9) and (11) that the amplitude of the perturbed pressure is

$$\frac{\partial P_1}{\partial \tau P_0} = \frac{\partial}{\partial \tau} \left( \frac{\rho_1}{\rho_0} + \frac{T_1}{T_0} \right) = -\Gamma \sum_{j=1}^3 V_j - \frac{1}{1 - (1 - \beta)\tau} \left( (2 - \beta) \frac{\rho_1}{\rho_0} - (1 - \beta) \frac{P_1}{P_0} \right). \quad (12)$$

## 2.2. The initially isochoric regime with $K \leq 1$

For computational simplicity, we now consider a 1-D limit treatment in which the initial (at  $\tau = 0$ ) amplitude of  $\rho_1$  equals to a finite value  $\rho_a$  with that of  $V_1$  and  $P_1$  equal to zero. These conditions correspond to an initially almost homogeneous, hot region of gas in pressure equilibrium. To third order in  $\tau$  the eqs (9), (10), and (12) give the following approximate solution

$$\frac{\rho_1}{\rho_0} \simeq \frac{\rho_a}{\rho_0} \left( 1 + \frac{K^2}{6} (2 - \beta) \tau^3 \right) \quad (13)$$

$$V \simeq \frac{(\beta - 2)K^2}{6} \frac{\rho_a}{\rho_0} (3\tau^2 + 2\beta\tau^3) \quad (14)$$

$$P \simeq (\beta - 2) \frac{\rho_a}{\rho_0} \left( \tau^2 + (1 - \beta) \tau^3 + \left( \frac{4}{3} - \frac{7}{3}\beta + \beta^2 - \frac{\Gamma K^2}{6} \right) \tau^3 \right) \quad (15)$$

Figure 1 compares this solution with a numerical integration of the complete non-linear hydrodynamical equations (1) to (3) for  $K=1$  and  $K=0.5$ . We use a 1-dimensional version of the second-order Eulerian hydro code which is described in Burkert and Bodenheimer (1993). The agreement between the numerical results (solid lines) and analytical solution (dots) is excellent, even for large values of  $\tau \approx 1$  where the basis of the analytic approximation is no longer valid.

Due to slightly more efficient cooling within the density perturbation a small pressure gradient builds up. In an attempt to maintain pressure balance, the slightly warmer gas in the low-density regions continually compresses the more dense and cooler parts. Consequently the over-density in the perturbed region increases as the gas cools. Figure 1 and the equations (13) to (15) show that for small values of  $K \leq 1$  the growth rate of the density enhancement depends on the size of the perturbation and increases with increasing values of  $K$  or decreasing wavelength. However, due to its long sound crossing timescale, the perturbation cannot be compressed significantly while cooling; it cools almost isochorically (Parker 1953). After one cooling timescale the gas temperature has reached its minimum value with the density enhancement still in the linear regime. Now, the pressure gradient reverses, erasing the fluctuation.

## 2.3. The initially isobaric regime: $K \geq 1$

The solid lines in figure 2 show a numerical calculation of the evolution of a density perturbation with  $K = 200$ ,  $\beta = 0$  and  $\Gamma = 5/3$ . For  $K \gg 1$ , perturbations can react quickly on any pressure gradients due to the short sound crossing timescale, relative to the cooling timescale. The simulations indicate a solution

which consists of a fast oscillatory part and a slowly growing part. Linearizing the slowly growing part, we find from the equations (9) to (12) the following approximate solution:

$$\frac{\rho_1}{\rho_0} \simeq \frac{\rho_a}{\rho_0} \left( \frac{i\omega\Gamma}{i\omega\Gamma - 2 + \beta} \right) \left( 1 + \frac{2 - \beta}{\Gamma} \left( \tau + \frac{i}{\omega} e^{i\omega\tau} \right) \right), \quad (16)$$

$$V \simeq \frac{\beta - 2}{\Gamma} \frac{\rho_a}{\rho_0} \left( \frac{i\omega\Gamma}{i\omega\Gamma - 2 + \beta} \right) (1 + i\omega\tau - e^{i\omega\tau}), \quad (17)$$

and

$$\frac{P_1}{P_0} \simeq \frac{(2 - \beta)i\omega}{\Gamma K^2} \frac{\rho_a}{\rho_0} \left( \frac{i\omega\Gamma}{i\omega\Gamma - 2 + \beta} \right) (1 + (1 - \beta)\tau - e^{i\omega\tau}). \quad (18)$$

The characteristic frequency is determined by a cubic dispersion relation

$$\omega^3 + i(1 - \beta)\omega^2 - K^2\Gamma\omega - i(2 - \beta)K^2 = 0. \quad (19)$$

A similar relation was discussed by Balbus (1995). Note that the linearized solution is also valid for  $\tau > 1/\omega$  as long as  $\tau \ll 1$ . As  $K \gg 1$  the two dominant real roots ( $\omega \approx \pm\sqrt{\Gamma}K$ ) of the dispersion eq(19) yield oscillatory parts in  $\rho_1/\rho_0$ ,  $V$ , and  $P_1/P_0$ . The upper panels of figure 2 show that for  $\tau < 0.1$  the analytical approximation is in good agreement with the numerical integration of the nonlinear hydrodynamical equations.

For all length scales, the ratio of sound propagation to cooling timescale

$$Q \equiv \tau_c(t)k\sqrt{R_g T_0(t)/\mu} = K(1 - (1 - \beta)\tau)^{\frac{3-2\beta}{2-2\beta}} \quad (20)$$

decreases during the subsequent evolution. Provided  $Q \gg 1$ , eq(18) implies that the magnitude of  $P_1/P_0$  is much smaller than both  $V$  and  $\rho_1/\rho_0$ . That is, the fluctuation reacts isobaric. Adopting  $P_1/P_0 \approx 0$  and neglecting the oscillatory term, the equations (9) and (12) can be combined to

$$-V = \frac{\partial}{\partial\tau} \left( \frac{\rho_1}{\rho_0} \right) = \frac{(2 - \beta)}{\Gamma(1 - (1 - \beta)\tau)} \frac{\rho_1}{\rho_0} \quad (21)$$

with the solution

$$\frac{\rho_1}{\rho_0} = \frac{\rho_a}{\rho_0} (1 - (1 - \beta)\tau)^{-\frac{2-\beta}{(1-\beta)\Gamma}} \quad (22)$$

and

$$V = -\frac{(2 - \beta)}{\Gamma} \frac{\rho_a}{\rho_0} (1 - (1 - \beta)\tau)^{-\frac{2-\beta}{(1-\beta)\Gamma}-1}. \quad (23)$$

In contrast to fluctuations with  $K < 1$  the evolution of isobaric fluctuations is independent of  $K$ . For  $(1 - \beta)^{-1} \gg \tau > \omega^{-1}$ , solutions for  $\rho_1/\rho_0$  in Eqs (16) and (22) are in agreement to first order in  $\tau$ . The lower panels of figure 2 show that within a cooling time both  $\rho_1/\rho_0$  and  $V$  are amplified to very large values. The agreement between the numerical calculation and the analytical prediction (equation 22 and 23) is excellent. The opposite signs of  $\rho_1/\rho_0$  and  $V$  confirm that mass is being pushed into the cool dense regions. For  $\tau \approx 1$ , the numerically derived density enhancement falls below the predicted values as the fluctuation becomes isochoric and contributions from the perturbed pressure cannot be neglected anymore.

#### 2.4. Transition to Isochoric Evolution and the Emergence of Small Scale Perturbations

Figure 3 shows the density evolution of initially isobaric fluctuations with different ratios of cooling to sound crossing times  $K$  as determined from the numerical calculations. The initially isobaric growth of the density fluctuations is independent of wavelength and  $K$  and in excellent agreement with equation (22) (dashed curve). The perturbations transform however to the isochoric solution for the epoch after  $Q$  has declined below unity. Thereafter, gas in the perturbed region cools off faster than it can adjust to a pressure equilibrium with the surrounding region. Subsequently, the over density of the perturbed region is slowly modified by the inertial motion  $V_{trans}$  of the gas at the time of the transition and its growth stalls. In Figure 3 the transition into the isochoric regime is indicated by the overdensity falling below the expected value shown by the dashed thick line.

Although the growth of the perturbed quantities does not explicitly depend on the wavelength  $k$ , the critical transition time when  $Q \approx 1$

$$\tau_{trans} = \frac{1 - K^{\frac{2\beta-2}{3-2\beta}}}{1 - \beta} \quad (24)$$

is a function of  $K$  (and  $k$ ). At this transition point, the over density in the perturbed region is

$$\frac{\rho_{trans}}{\rho_0} = \frac{\rho_a}{\rho_0} K^{\frac{(4-2\beta)}{(3-2\beta)\Gamma}}. \quad (25)$$

and the velocity is

$$V_{trans} = -\frac{2 - \beta}{\Gamma} \frac{\rho_a}{\rho_0} K^{(\frac{2-2\beta}{3-2\beta})(1 + \frac{2-\beta}{(1-\beta)\Gamma})}. \quad (26)$$

In the isochoric regime the amplitude of the perturbed density increases as

$$\frac{\rho_1}{\rho_0} = \frac{\rho_{trans}}{\rho_0} - V_{trans} * (\tau - \tau_{trans}) \quad (27)$$

which increases much less steeply than the isobaric fluctuations (equation 22).

For thermally unstable clouds,  $\beta < 1$  such that  $\rho_{trans}/\rho_0$  is an increasing function of  $K$  or a decreasing function of the wavelength ( $\lambda$ ) of the perturbations. Despite the independence of the rate of change of  $\rho_1/\rho_0$  on  $\lambda$ , equation 24 shows that for  $\beta < 1$  the short length scale disturbances undergo isobaric to isochoric transition at a later time and therefore acquire a greater limiting amplitude than the long length scale disturbances. Thus, the short length scale disturbances would emerge to dominate the structure of the cloud unless the initial perturbation amplitude  $\rho_a/\rho_0$  increases with  $K$  more rapidly than  $K^{(2\beta-4)/(3-2\beta)\Gamma}$ . This evolution is physically equivalent to the fragmentation process in which the contrast between the enhanced density in a disturbance and the average cloud density becomes most pronounced on the smallest scales.

### 3. The Transition into the Nonlinear Regime

In Fig. 3 fluctuations with very large values of  $K$  show yet another evolution: for later times the overdensity rises faster than predicted by equation (22). These fluctuations become nonlinear with  $\rho_1/\rho_0 > 1$  before the transition into the isochoric regime. The critical value of  $K$  for this evolution can be estimated from equation (25) assuming  $\rho_{trans}/\rho_0 = 1$ :

$$K_{crit} = \left( \frac{\rho_a}{\rho_0} \right)^{\frac{(2\beta-3)\Gamma}{4-2\beta}} \quad (28)$$

For  $K > K_{crit}$  the analytical approximations discussed previously are not valid anymore and we have to investigate the evolution numerically, solving the complete non-linear hydrodynamical equations. The simulations shown in figure 3 assumed  $\beta = 0$ ,  $\Gamma = 5/3$  and  $\rho_a/\rho_0 = 10^{-3}$ . For these values the simple approximation (28) predicts  $K_{crit} = 5600$  which is roughly in agreement with the numerical results where the transition into the nonlinear regime occurs more smoothly between  $K=1000$  and  $K=5000$ . Equation (28) somewhat overestimates  $K_{crit}$  because nonlinear effects actually become important earlier, when the overdensity is in the range  $0.1 < \rho_1/\rho_0 < 1$ .

Figure 4 shows the structure and evolution of a non-linear fluctuation. During the early isobaric evolution the pressure gradient (lower right panel) is negligible. A small pressure gradient builds up in

the nonlinear regime, where the profiles cannot be approximated anymore by sinusoidal functions but instead become strongly peaked towards the center. Non-linear fluctuations grow fast with the density and temperature reaching their maximum and minimum values, respectively, at a time  $\tau_{crit} < 1$  which is shorter than a cooling time. Due to the fast growth in the nonlinear regime,  $\tau_{crit}$  is roughly given by the time when  $\rho_1/\rho_0 = 1$ . From Eq (22), we find

$$\tau_{crit} = \frac{1}{1-\beta} \left( 1 - \left( \frac{\rho_a}{\rho_0} \right)^{\frac{(1-\beta)\Gamma}{2-\beta}} \right). \quad (29)$$

At  $t = \tau_{crit}$ , the dimensionless velocity (see Eq. 23)

$$V_{crit} = V(\tau_{crit}) = \frac{\beta - 2}{\Gamma} \left( \frac{\rho_a}{\rho_0} \right)^{-\Gamma \frac{1-\beta}{2-\beta}} \quad (30)$$

is much larger than unity for perturbations with small initial amplitudes such that contributions due to nonlinear advection (such as  $U_j \partial \rho / \partial x_j$ ,  $U_j \partial U_j / \partial x_j$ , and  $U_j \partial T / \partial x_j$ ) would exceed the linear contributions contained in the perturbed equations (6-8) before the over density  $\rho_1$  has become comparable to  $\rho_0$  (see above). Advection generally enhances the effect of compression and promotes the growth of density contrast at an accelerated rate.

Although the time of maximum compression for a fluctuation with  $K > K_{crit}$  does not depend explicitly on the length scale, it is determined by the initial amplitude  $\rho_a/\rho_0$  of the perturbation which may be a function of the wavelength. For an initial power-law perturbation in which  $\rho_a/\rho_0 = A_0(k/k_0)^\eta$ ,

$$\tau_{crit} = \frac{1}{1-\beta} \left( 1 - \left( A_0 \frac{k}{k_0} \right)^{\frac{(1-\beta)\Gamma\eta}{2-\beta}} \right). \quad (31)$$

If the amplitude of the initial perturbation is an increasing function of the wavelength (which corresponds to a negative  $\eta$ ),  $\tau_{crit}$  would be an increasing function of  $k$  in the thermally unstable region with  $\beta < 1$ . In this case, nonlinearity would be first reached on the largest length scale with  $K > K_{crit}$ . If, however, the amplitude of the initial perturbation is a decreasing function of the wavelength (*i.e.*  $\eta > 0$ ),  $\tau_{crit}$  would be a decreasing function of  $k$  and nonlinearity would be reached on the smallest scale first. Note that for  $1 < \beta < 2$ , the dependence of  $\tau_{crit}$  on  $\eta$  and  $k$  is reversed.

In Figure 3, a temperature independent cooling function has been used. In order to determine the dependence on the specific form of the cooling function, additional simulations have been performed, adopting a more realistic cooling function (Dalgarno & McCray 1972) which assumes solar element abundance and collisional equilibrium ionization. Note that for temperatures  $T > 10^4$  K the cooling rate

is several orders of magnitudes larger than for  $T < 10^4$  K, defining two different temperature regimes with very different cooling timescales. The simulations show that the previous results remain valid for each of these temperature regimes. Starting in the low-temperature regime, a fluctuation will become non-linear for  $K > K_{crit}$  and cool down to the lowest allowed temperature. The same is true for fluctuations that start in the high-temperature regime. Non-linear fluctuations in this regime do however stop cooling efficiently at  $T \approx 10^4$  K, leading to high-density clumps with such a temperature.

#### 4. Interacting Fluctuations and the Emergence of Substructure with a Critical Wave Length

Up to now we have investigated the evolution of isolated fluctuations. In reality however a cooling gaseous region consists of a superposition of fluctuations with different wavelengths and amplitudes. As we indicated in the previous section, the outcome of the thermal instability may be determined by the wavelength dependence in the initial amplitude of the perturbations.

In order to illustrate various competing effects such as isobaric to isochoric transition and the onset of nonlinear growth, we present in Figure 5 a series of models with  $\beta = 0$  and  $\Gamma = 5/3$ , where the initial density distribution consists of the superposition of two fluctuations with ratios of wavelengths  $\lambda_1/\lambda_2 = 20$  and amplitude ratios  $\rho_{a,1}/\rho_{a,2} = 2$  which corresponds to  $\eta = -0.23$ . Four values of  $\lambda_1$  were chosen and they correspond to  $K_1=1,10,100$  and  $1000$ , respectively. The  $K_2$  values for the smaller perturbation are always a factor 20 larger. Since the initial overdensity  $\rho_{a,1}/\rho_0 = 0.01$ , the critical value of  $K$  for nonlinear evolution is  $K_{crit} = 316$ , according to equation (28). We show the density distribution after  $1 \tau_c(0)$ . In the upper left panels of Fig. 5, the fluctuations have values of  $K_1 = 1$  and  $K_2 = 20$  which are small compared to  $K_{crit}$ . Their growth therefore stalls due to transition into the isochoric regime and the overdensity after a cooling time is still linear. The smaller fluctuation dominates at the end because its isochoric transition occurs later and at a higher overdensity than for the larger perturbation. In the upper right panels with  $K_1 = 10$  and  $K_2 = 200$  the smaller perturbation is again dominating after  $\tau = 1$  although, now, the density distribution is also affected by the underlying larger perturbation. In both cases the density within the density peaks does not decrease much with respect to its initial value. The situation is different in the lower left panel with  $K_1 = 100$  and  $K_2 = 2000$ . Here the smaller perturbation has become nonlinear, generating small dense clumps which stand out against the larger perturbation. Up to now, the smaller perturbation was always dominating the density distribution after a cooling time. The situation is however different in the lower right panel where  $K_1 > K_{crit}$ . Now, the larger perturbation becomes nonlinear and advection

drives all the gas and its small scale fluctuations into one very dense, cold clump that is embedded in a hot diffuse environment, erasing smaller scale fluctuations.

The dependence of structure formation on the initial power-law perturbation index  $\eta$  is illustrated in figure 6 which shows the initial and final density distribution of two interacting perturbations with  $\lambda_1/\lambda_2 = 10$ ,  $K_1 = 2 \times 10^4$ ,  $\rho_{a,1}/\rho_{a,2} = 10$  ( $\eta = -1$ ) in the left panels and  $\rho_{a,1}/\rho_{a,2} = 0.1$  ( $\eta = 1$ ) in the right panels. As expected, in the case of  $\eta = -1$  the larger perturbation becomes nonlinear first, leading to one massive density peak after a cooling time. For  $\eta = 1$ , the small length scale perturbations begin to dominate after a cooling time, breaking the region up into dense clumps on the smallest scale. More specifically, if the amplitude of the initial perturbation increases with increasing wavelength ( $\eta < 0$ ), clumps will form with length scales  $\lambda \approx \lambda_{crit}$ . Otherwise, the sizes of the fastest growing perturbations will be  $\lambda \approx \lambda_\kappa$ . In this case, the clump sizes should decrease with increasing magnetic field strength.

## 5. The importance of thermal conduction

During the growth of linear density perturbations in the isobaric regime the resulting temperature gradient will induce conductive heating of the fluctuations.

### 5.1. Thermal conduction in the absence of magnetic fields

Several studies (e.g. McKee & Begelman 1990, Ferrara & Shchekinov 1993) have demonstrated that thermal conduction could stabilize and even erase a density perturbation if its scale is smaller than the Field length (Field 1965)

$$\lambda_F = \left( \frac{\kappa T}{n^2 \Lambda} \right)^{1/2} \quad (32)$$

where  $\kappa$  is the thermal conduction coefficient.

In order to include the effect of thermal conduction, the term  $\nabla(\kappa \nabla T)/\rho C_v$  has to be added to the right-hand side of equation (3). The linearized pressure equation (12) is then

$$\frac{\partial}{\partial \tau} \frac{P_1}{P_0} = -\Gamma \sum_{j=1}^3 V_j - \frac{1}{1 - (1 - \beta)\tau} \left( (2 - \beta) \frac{\rho_1}{\rho_0} - (1 - \beta) \frac{P_1}{P_0} \right) - \frac{\kappa}{\rho_0 C_v} \frac{T_1}{T_0} k^2 \tau_c(0). \quad (33)$$

In the isobaric regime with  $P_1/P_0 \approx 0$  and  $T_1/T_0 \approx -\rho_1/\rho_0$  thermal conduction will become important if

$$\frac{\kappa}{\rho_0 C_v} k^2 \tau_c(0) \geq \frac{2 - \beta}{1 - (1 - \beta)\tau} \quad (34)$$

In the early stages of cooling ( $\tau \ll 1$ ) fluctuations will therefore be erased by thermal conduction if their wavelengths are

$$\lambda \leq \lambda_\kappa = \frac{2\pi}{(2 - \beta)^{1/2}} \lambda_F. \quad (35)$$

Figure 7 shows the evolution of an initially isobaric, 1-dimensional fluctuation with a ratio of cooling-to sound crossing time  $K=200$  and  $\beta = 0$ . The 1-dimensional, non-linear hydrodynamical equations (1) - (3) are solved numerically, including thermal conduction. The solid line shows the evolution of the density contrast  $\rho_1/\rho_0$  as predicted by the analytical model (equation 22) which is in excellent agreement with the numerical result (filled points) for  $\lambda > \lambda_\kappa$ . For  $\lambda = \lambda_\kappa$  (upper dashed line) conductive heating is non-negligible anymore and the fluctuation grows less fast. For  $\lambda < \lambda_\kappa$  the growth of fluctuations is suppressed by thermal conduction.

In summary, thermal conduction can play a significant role in regulating the break-up of a radiatively cooling gaseous medium. Small scale substructure can only emerge in a limited wavelength regime which is given by

$$\lambda_\kappa \leq \lambda \leq \lambda_{crit} \quad (36)$$

The growth of perturbations is completely suppressed if  $\lambda_{crit} < \lambda_\kappa$  for all perturbations.

The dotted lines in figure 8a show  $\lambda_{crit}$  for fluctuations with initial overdensities  $\log(\rho_a/\rho_0) = -3, -2, -1$ , the solid line shows  $\lambda_\kappa$ . A cooling function assuming collisional equilibrium ionization (Spitzer 1978, Dalgarno & McCray 1972) and a realistic conduction coefficient (Ferrara & Shchekinov 1993) has been adopted. The dashed line shows the mean free path (Cowie & McKee 1977)

$$\lambda_e \approx 10^4 \left( \frac{T}{K} \right)^2 \left( \frac{cm^{-3}}{n} \right) cm \quad (37)$$

for electron energy exchange. Note that for a given temperature the ratios  $\lambda_\kappa/\lambda_{crit}/\lambda_e$  are independent of pressure.

The classical thermal conductivity is based on the assumption that  $\lambda_e$  is short compared to the temperature scale height  $h_T \approx \lambda/(T_1/T_0) > \lambda_{crit}$ . Otherwise, the heat flux  $q$  is saturated (Cowie & McKee 1977) and no longer equal to  $q = -\kappa\nabla T$ . Indeed, figure 8a shows that linear fluctuations in astrophysical plasmas will in general lie in the non-saturated regime ( $\lambda_{crit} > \lambda_e$ ) for initial amplitudes  $\rho_a/\rho_0 \geq 0.001$ .

However, we also find that in general  $\lambda_\kappa > \lambda_{crit}$  for perturbations with amplitudes  $\log(\rho_a/\rho_0) \leq -2$ . This implies that a cooling instability, resulting from linear density perturbations will in general be suppressed by thermal conduction.

## 5.2. Thermal conduction, including magnetic fields

The interstellar medium is in general penetrated by magnetic fields. In most situations the electron mean free path  $\lambda_e$  is large compared to the length scale at which the resistive destruction of the magnetic field is significant. A tangled magnetic field can then develop, concentrated on scales  $l_B$  which are smaller than  $\lambda_e$  (Chandran & Cowley 1998). When the gyroradius

$$a = \frac{v_T m_e c}{eB} \approx 2.2 \times 10^8 \sqrt{\frac{T}{10^8 K}} \left( \frac{\mu G}{B} \right) cm \quad (38)$$

of thermal electrons with typical velocities  $v_T = (kT/m_e)^{1/2}$  is much smaller than  $l_B$  or  $\lambda_e$  the magnetic field controls the motion of individual electrons. This condition is satisfied in many astrophysical plasmas even if the magnetic field is too weak to be hydrodynamically important.

If  $a$  is small compared to the length scale  $\lambda$  of a fluctuation, heat is conducted according to the classical thermal conduction equation (Spitzer 1962), however with a thermal conductivity  $\kappa_B$  which is reduced from the classical Spitzer value  $\kappa$  as a result of the tangled magnetic field by (Chandran & Cowley 1998)

$$\kappa_B \approx \frac{0.1}{\ln(l_B/a)} \kappa. \quad (39)$$

If we normalize  $B$  to its value for magnetic-to-thermal energy equipartition  $B_T = (24\pi\rho R_g T)^{1/2}$  we find

$$\ln\left(\frac{l_B}{a}\right) = -3.1 + \ln\left(\frac{B}{B_T}\right) + 2\ln\left(\frac{T}{K}\right) - 0.5\ln\left(\frac{n}{\text{cm}^{-3}}\right) + \ln\left(\frac{l_B}{\lambda_e}\right). \quad (40)$$

For weak magnetic fields ( $B \approx 0.01B_T$ ) and length scales  $l_B$  of order the electron mean free path equation 40 leads to  $\ln(l_B/a) \geq 10$ , by this reducing  $\kappa_B$  by two orders of magnitudes and the length scale of thermal conduction by one order of magnitude. As an example, the shaded area in figure 8b shows the wavelength regime  $\lambda_\kappa \leq \lambda \leq \lambda_{crit}$  where linear fluctuations with  $\rho_a/\rho_0 = 10^{-2}$  could grow as a result of cooling, assuming a pressure of  $P/k_B = 10^3 \text{ K cm}^{-3}$  and  $l_B = 0.1\lambda_e$ . The presence of a weak magnetic field can suppress thermal conduction efficiently, allowing small scale structure with wavelengths  $\lambda \approx 10^{-2} \text{ pc}$  to emerge as a result of cooling.

## 6. The importance of heating and the emergence of a stable two-phase medium.

The calculations in sections 3 and 4 showed that cooling gas clouds with small initial perturbations break up on a critical wave length  $\lambda_{crit}$  below which over density first becomes nonlinear. If the initial amplitude is a decreasing function of  $\lambda$ , the clouds would break up on the smallest length where the local radiative cooling law remains valid and fluctuations are not destroyed by conduction. But, if the initial amplitude is an increasing function of the wavelength,

$$\lambda_{crit} = \frac{2\pi\tau_c(0)}{K_{crit}} \sqrt{\frac{R_g T_0(0)}{\mu}}. \quad (41)$$

small perturbations on scales  $\lambda < \lambda_{crit}$  are erased when the gas accumulates in the center of fluctuations with  $\lambda = \lambda_{crit}$ . Perturbations with  $\lambda > \lambda_{crit}$  do not become nonlinear but they break up into substructures with  $\lambda = \lambda_{crit}$ .

After a cooling time the dense, cold, non-linear perturbations are embedded in a warmer, diffuse environment (see Fig. 9). However, the example in figure 9 shows that the cooling timescale of the inter-clump gas remains short compared to the initial cooling timescale. This gas therefore cools to a ground state temperature  $T_{min}$  shortly after  $\tau = 1$ . Subsequently the reversed pressure gradient would remove the fluctuations unless they are gravitationally bound.

In order to maintain a stable two-phase medium a heating term must be included (Field et al. 1969). Here we assume a power law dependence of the heating rate

$$\Gamma_h = \Gamma_0 \rho^\gamma \tag{42}$$

where  $\Gamma_0$  and  $\gamma$  are constants. In general, the size of the whole cooling region is large compared to  $\lambda_{crit}$  such that it cannot establish pressure equilibrium with the surrounding confining medium during a cooling timescale. In this case, the region cools isochorically and breaks up into substructures on scales of  $\lambda_{crit}$  before establishing pressure equilibrium with the environment. If the average gas density  $\rho_0$  is smaller than a critical value

$$\rho_\Gamma = \left( \frac{\Gamma_0}{\Lambda_0} T^{-\beta} \right)^{\frac{1}{2-\gamma}} \tag{43}$$

heating would dominate everywhere and the region would adjust to a thermal equilibrium state where heating is balanced against cooling. If  $\rho_0 > \rho_\Gamma$  cooling dominates and the density fluctuations would grow and become non-linear as discussed in the previous sections. Eventually, after a cooling time, the region would break up into cold high-density condensations which are separated by warm gas with densities  $\rho_{min} \ll \rho_0$ . If  $\rho_{min} > \rho_\Gamma$  this interclump medium would cool as shown in figure 9 and the density fluctuations would be erased. Figure 10 shows a situation with  $\rho_{min} < \rho_\Gamma$ . Heating dominates in the interclump region where the gas temperature and gas pressure rise, until pressure equilibrium is established. A stable 2-phase medium has formed with cold clouds of minimum temperature embedded in a hot interclump medium with a temperature that is determined by the balance of cooling and heating.

## 7. Discussions

The discussions in this paper focussed on the emergence of small scale perturbations. We have assumed the pre-existence of small initial perturbations which is a reasonable assumption for dynamically evolving systems like the interstellar medium in galaxies or in galactic clusters. We have limited our analysis to the optically thin regime such that radiation transfer is solely due to optically thin local radiative processes. This approximation is appropriate for the collapse of supercritical clouds where the effect of a magnetic field is dominated by thermal processes. Such a situation may be particularly relevant for the formation of stellar clusters and first generation stars in galaxies. Provided that the density of the progenitor clouds is relatively small, the local cooling approximation is adequate. We also neglected the interaction and merging of clumps. These processes become important for the subsequent evolution and they will be considered in

subsequent papers.

In the context of our approximations, we have shown that thermal instability can lead to the breakup of large clouds into cold, dense clumps with a characteristic length scale which is given by  $\lambda_{crit}$  in eq. (41) or by the smallest unstable wavelength that is not erased by thermal conduction, depending on whether the amplitude of the initial perturbation is an increasing or decreasing function of wavelength. For linear perturbations with overdensities  $\rho_a/\rho_0 \approx 0.01$  the critical wavelength lies in the regime of  $10^{-3}$  pc to  $10^{-1}$  pc, depending on the initial temperature. The emergence of small scale dense subcondensations is equivalent to fragmentation. As in a thermally unstable region the cooling timescale is shorter than the dynamical timescale, gravity has no time to play an important role during this fragmentation process.  $\lambda_{crit}$  may be either smaller or bigger than the Jeans' length. In the latter case gravity becomes important eventually. In general however, thermally induced fragmentation of clouds with small initial density fluctuations proceeds the onset of gravitational instability of their individual clumps.

In our analyses, we adopted an idealized power-law cooling function. In reality, the cooling efficiency would terminate when the main cooling agents reach their ground state or establish an equilibrium with some external heating source. The latter is necessary for the clouds to attain a two-phase medium. Interaction between these two phases may determine the pressure, density and infall rate of the cloud complex as well as the dynamical evolution and size distribution of cloudlets and sub condensations. The analysis of this interaction will be presented elsewhere.

We would like to thank the referee, Andrea Ferrara, for helpful suggestions and for pointing out the importance of thermal conduction. A. Burkert thanks the staff of UCO/Lick Observatory for the hospitality during his visits. We thank S.D. Murray for useful conversation. This research was supported by NASA through NAG5-3056, and an astrophysics theory program which supports a joint Center for Star Formation Studies at NASA-Ames Research Center, UC Berkeley, and UC Santa Cruz.

## REFERENCES

- Arons, J. & Max, C.E. 1975, *ApJ*, 196, L77
- Balbus, S.A. 1986, *ApJ*, 303, L79
- Balbus, S.A. 1995, *The Physics of the Interstellar Medium and Intergalactic Medium*, ASP Conf. Ser. 80, eds. A. Ferrara, C.F. McKee, C. Heiles & P.R. Shapiro, p. 328
- Blitz, L. 1993, *Protostars and Planets III*, eds. E.H. Levy & J.I. Lunine, p. 125
- Blumenthal, G.R., Faber, S.M., Primack, J.R. & Rees, M.J. 1984, *Nature*, 311, 517
- Brown, J.H., Burkert, A., Truran, J.W. 1991, *ApJ*, 376, 115
- Brown, J.H., Burkert, A., Truran, J.W. 1995, *ApJ*, 440, 666
- Burkert, A. & Bodenheimer, P. 1993, *MNRAS*, 264, 798
- Burkert, A. & Bodenheimer, P. 1996, *MNRAS*, 280, 1190
- Burkert, A., Bate, M. & Bodenheimer, P. 1997, *MNRAS*, 289, 497
- Carpenter, J.M., Meyer, M.R., Dougados, C., Strom, S.E. & Hillenbrand, L.A. 1997, *AJ*, 114, 198
- Chandran, B.D.G. & Cowley, S.C. 1998, *Phys. Rev. Lett.*, 80, 3077
- Cowie, L.L. & McKee, C.F. 1977, *ApJ*, 211, 135
- Crutcher, R.M., Troland, T.H., Goodman, A.A., Heiles, C., Kazes, I. & Myers, P.C. 1993, *ApJ*, 407, 175
- Dalgarno, A. & McCray, R.A. 1972, *Ann. Rev. Astron. Astroph.*, 10, 375
- Ferrara, A. & Shchekinov, Y. 1993, *ApJ*, 417, 595
- Field, G.B. 1965, *ApJ*, 142, 531
- Field, G.B., Goldsmith, D.W. & Habing, H.J. 1969, *ApJ*, 155, L49
- Franco, J., & Cox, D.P. 1983, *ApJ*, 273, 24
- Gammie, C.F. & Ostriker, E.C. 1996, *ApJ*, 466, 814

- Hillenbrand, L.A. 1997, *AJ*, 113, 1733
- Hunter, C. 1962, *ApJ*, 136, 594
- Kraft, R.P. 1979, *ARAA*, 17, 309
- Larson, R.B. 1981, *MNRAS*, 194, 809
- Lin, D.N.C. & Murray, S.D. 1992, *ApJ*, 394, 523
- Lizano, S. & Shu, F.H. 1989, *ApJ*, 342, 834
- Loewenstein, M. 1990, *ApJ*, 349, 471
- MacLow, M.M., Klessen, R.S., Burkert, A., Smith, M.D. & Kessel, O. 1998, *Phys. Rev. Lett.*, 80, 2754
- MacLow, M.M. 1999, *ApJ*, in press
- McKee, C.F. 1989, *ApJ*, 345, 782
- McKee, C.F. & Begelman, M.C. 1990, *ApJ*, 358, 392
- Mouschovias, T.C. & Spitzer, L.H. 1976, *ApJ*, 210, 326
- Mouschovias, T.C. 1991, *ApJ*, 373, 169
- Murray, S.D. & Lin, D.N.C. 1992, *ApJ*, 400, 265
- Myers, P.C. & Goodman, A.A. 1988, *ApJ*, 326, L27
- Nakano, T. 1979, *PASJ*, 31, 697
- Parker, E.N. 1953, *ApJ*, 117, 431
- Schwarz, J., McCray, R. & Stein, R. 1972, *ApJ*, 175, 673
- Shu, F., Najita, J., Galli, D., Ostriker, E. & Lizano, S. 1993, *Protostars and Planets III*, eds. E.H. Levy & J.I. Lunine, p.3
- Solomon, P.M., Rivolo, A.R., Barrett, J. & Yahil, A. 1987, *ApJ*, 319, 730
- Spitzer, L. 1962, *Physics of Fully Ionized Gases* (New York: Interscience Publishers).

- Spitzer, L. 1978, *Physical Processes in the Interstellar Medium* (New York: Wiley). s of Fully Ionized,  
Solomon, P.M., Rivolo, A.R., Barrett, J. & Yahil, A. 1987, *ApJ*, 319, 730
- Ostriker, E.C., Gammie, C.F. & Stone, J.M. 1999, *ApJ*, 513, 259

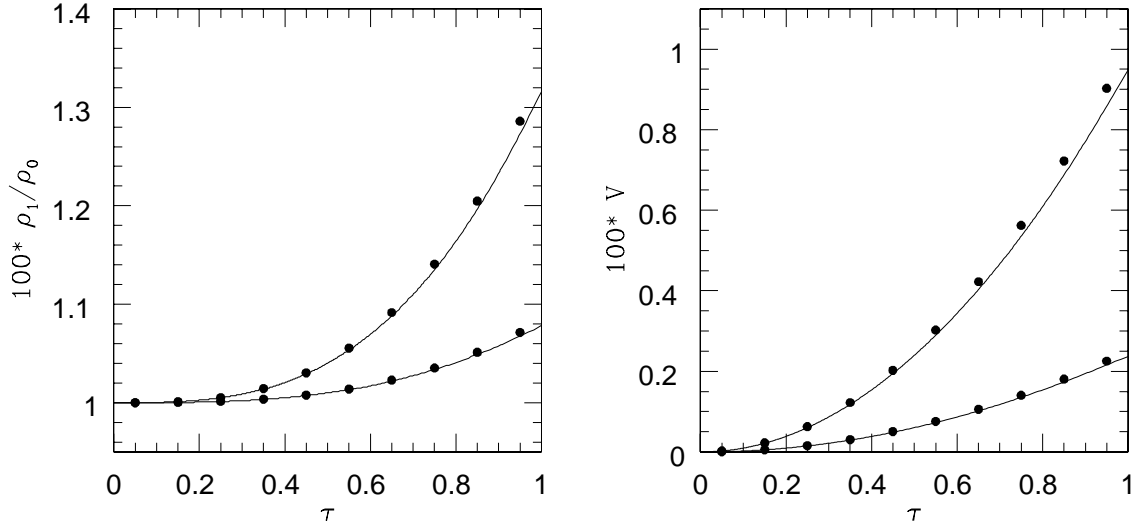


Fig. 1.— The solid lines show the numerical results of the evolution of the overdensity (left panel) and dimensionless velocity (right panel) for almost isochoric perturbations with  $K=1$  (upper curves) and  $K=0.5$  (lower curves). A cooling law with  $\beta = 0$  is adopted. The dots represent the analytical solution (equations 13 and 14).

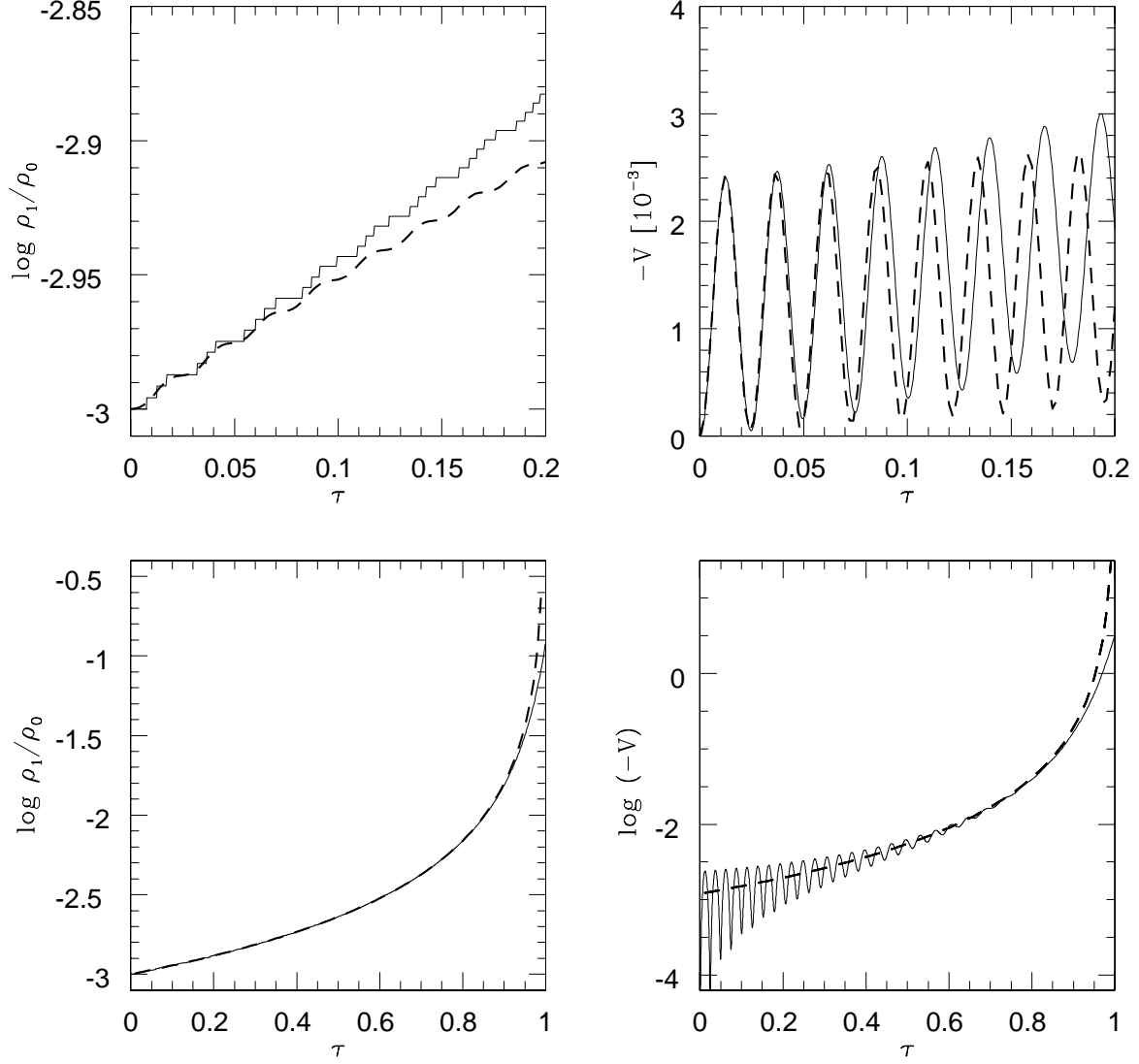


Fig. 2.— The growth of an initially isobaric density perturbation with  $K=200$  is shown, adopting  $\beta = 0$  and  $\Gamma = 5/3$ . The numerical results (solid lines) are compared with the analytical solutions (dashed curves). The upper two panels show the early evolution which is compared with the predictions of the linearized equations (16) and (17) assuming  $\omega = \sqrt{\Gamma}K$ . The lower panels show the evolution till  $\tau = 1$  which is compared with the results of the nonlinear equations (22) and (23).

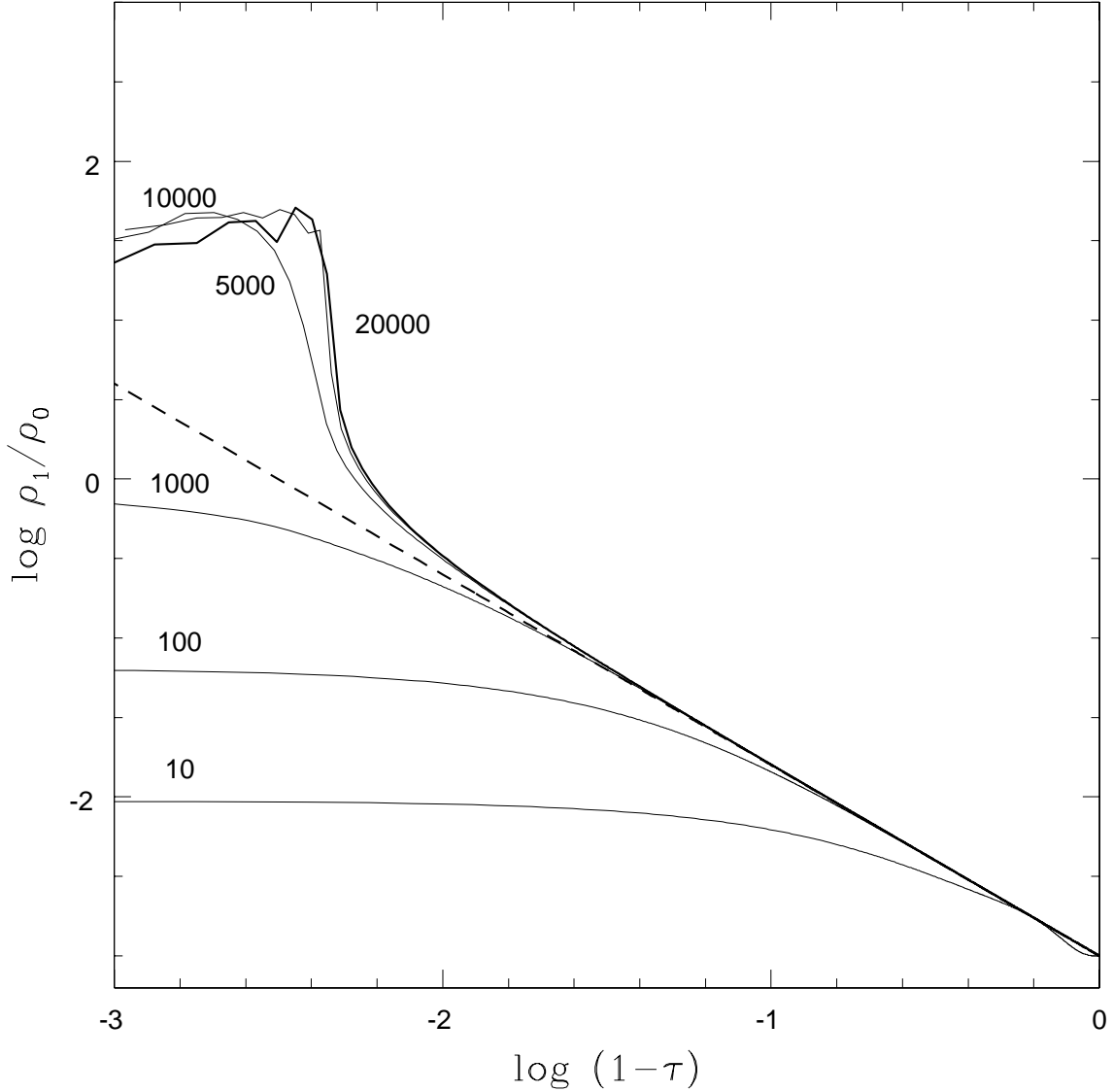


Fig. 3.— The growth of initially isobaric fluctuations is shown. The solid curves, labeled by the adopted initial  $K$ -values of the fluctuations show the results of numerical calculations for  $\beta = 0$ . The thick dashed line shows the evolution of a linear isobaric perturbation as predicted by equation (22). Fluctuations with small values of  $K$  become isochoric and their density increase stalls. Above a critical value of  $K$  fluctuations become nonlinear during their isobaric growth. These fluctuations evolve faster than predicted by the linear approximation and achieve very large density contrasts on a timescale which is independent of  $K$  and shorter than a cooling timescale.

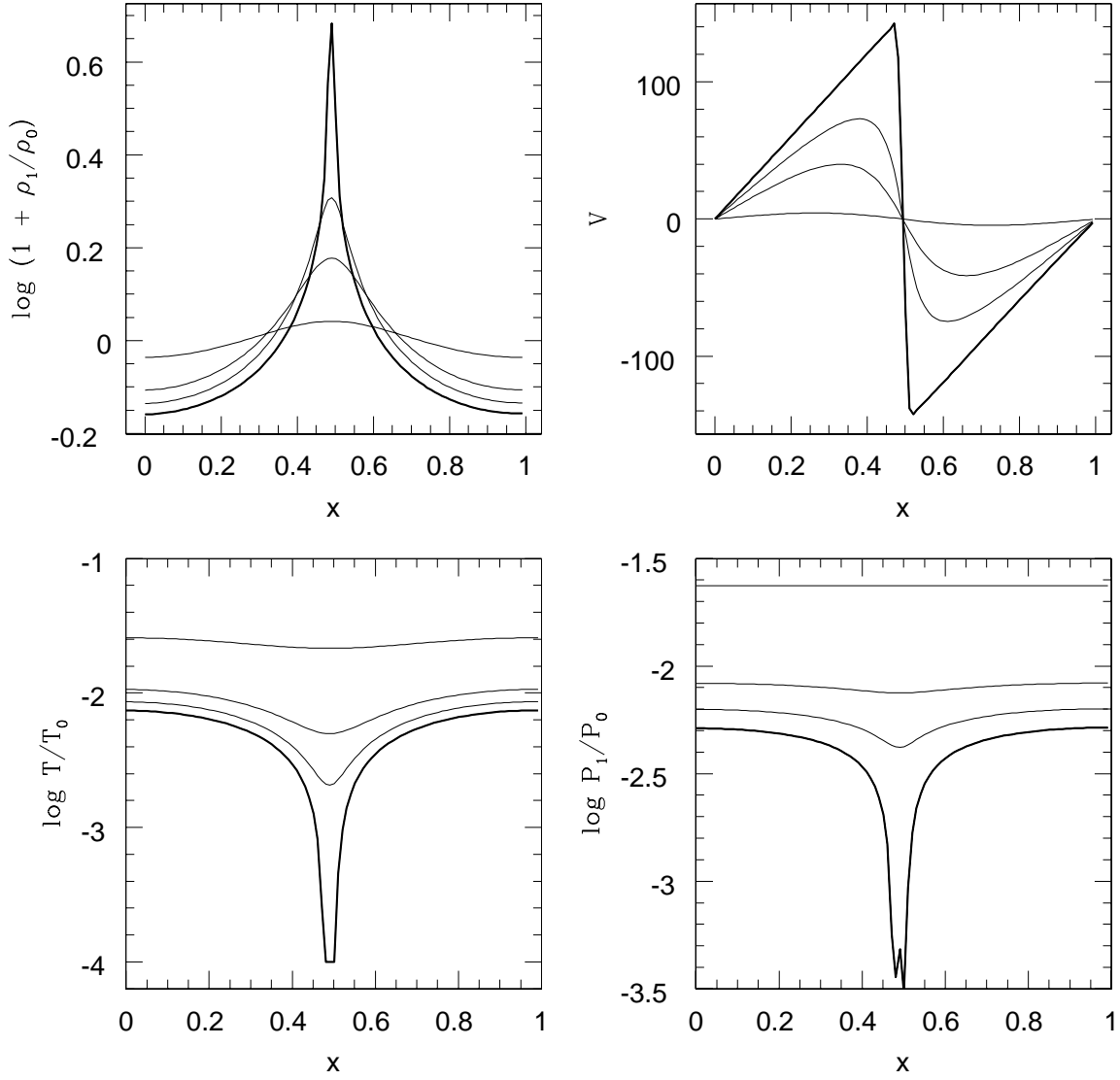


Fig. 4.— The evolution of overdensity  $\rho_1/\rho_0$ , dimensionless velocity  $V$ , temperature  $T_1/T_0$  and pressure  $P_1/P_0$  of a nonlinear fluctuation with  $K=1000$ , assuming  $\beta = 0$ . Cooling is assumed to stop after the temperature has decreased by 4 orders of magnitude. The evolutionary state of the system is shown at the time when the overdensity is 0.1, 0.5, 1 and 5 times the initial density.

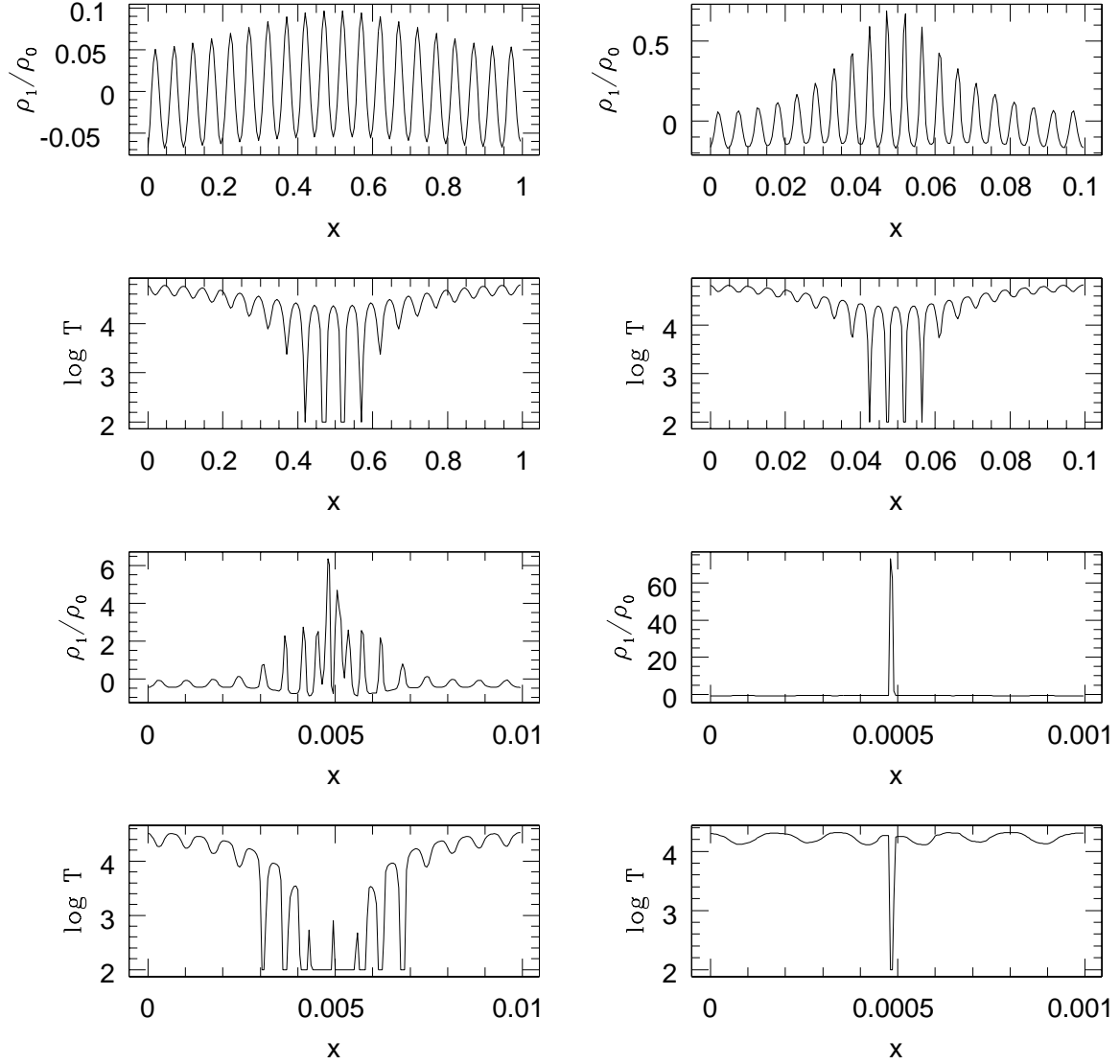


Fig. 5.— The figures show the overdensity and the temperature distribution after a cooling time of regions with two interacting fluctuations with wavelength ratios  $\lambda_1/\lambda_0 = 20$  and amplitude ratios  $\rho_{a,1}/\rho_{a,2} = 0.5$ , adopting different values of  $K$ . The  $x$ -coordinate is normalized to the wavelength of a perturbation with  $K=1$ .

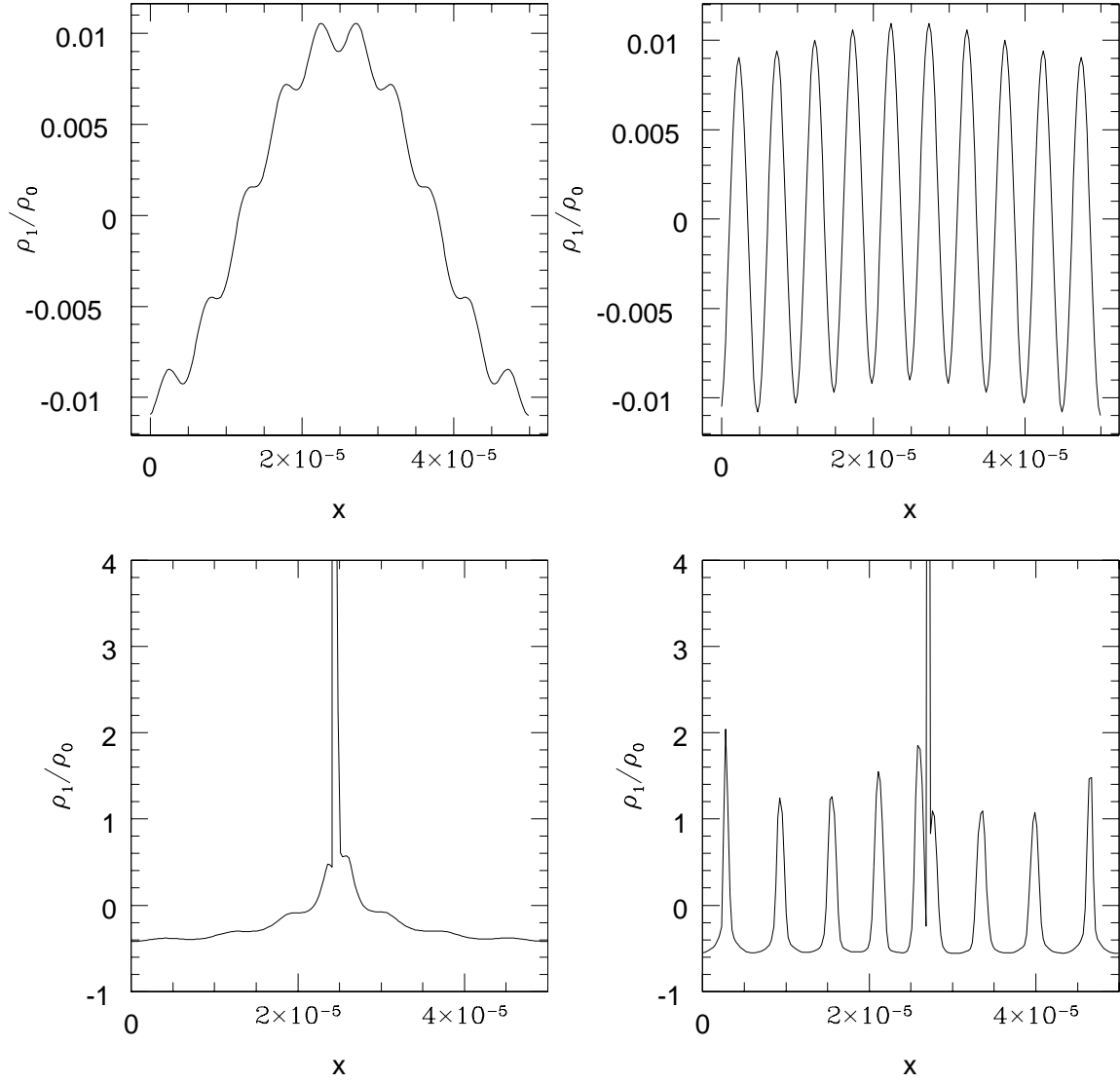


Fig. 6.— The left upper and lower panels show, respectively, the initial ( $\tau = 0$ ) and final ( $\tau = 1$ ) density distribution of two nonlinear interacting density perturbations with  $\lambda_1/\lambda_0 = 10$  and  $\eta = -1$ . The initial and final density distributions for interacting nonlinear fluctuations with  $\eta = 1$  are shown, respectively, in the upper and lower right panels.

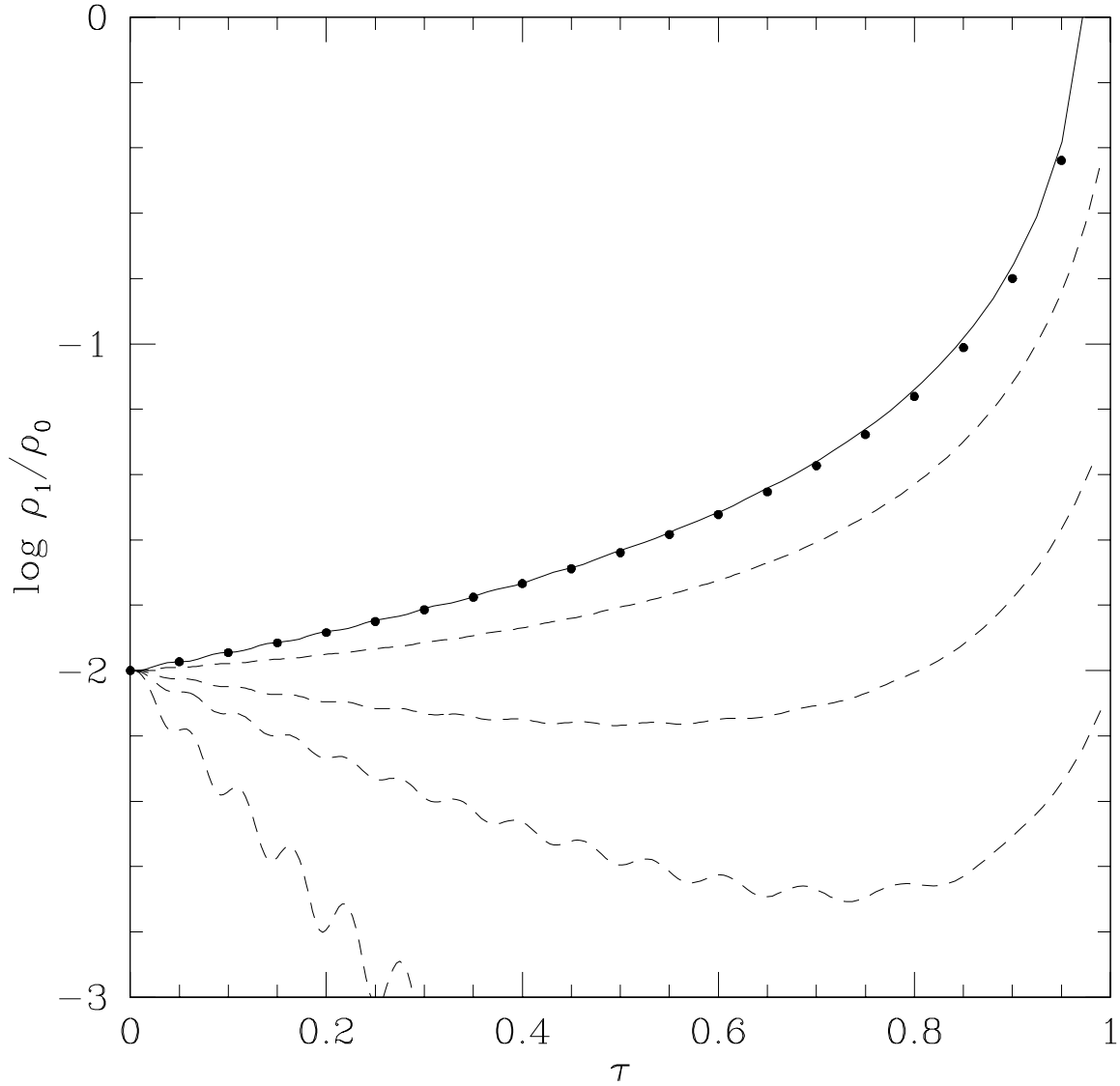


Fig. 7.— The effect of thermal conduction on the growth of a perturbation with  $\rho_a/\rho_0 = 0.01$  and  $K = 200$  is shown, adopting a cooling function with  $\beta = 0$ . The solid thick line shows the theoretical prediction and the filled points show the numerical result for  $\lambda_\kappa = 0$ . The lower dashed lines show the evolution of fluctuations with  $\lambda = \lambda_\kappa$ ,  $\lambda = 0.75\lambda_\kappa$ ,  $\lambda = 0.5\lambda_\kappa$ , and  $\lambda = 0.25\lambda_\kappa$ , respectively.

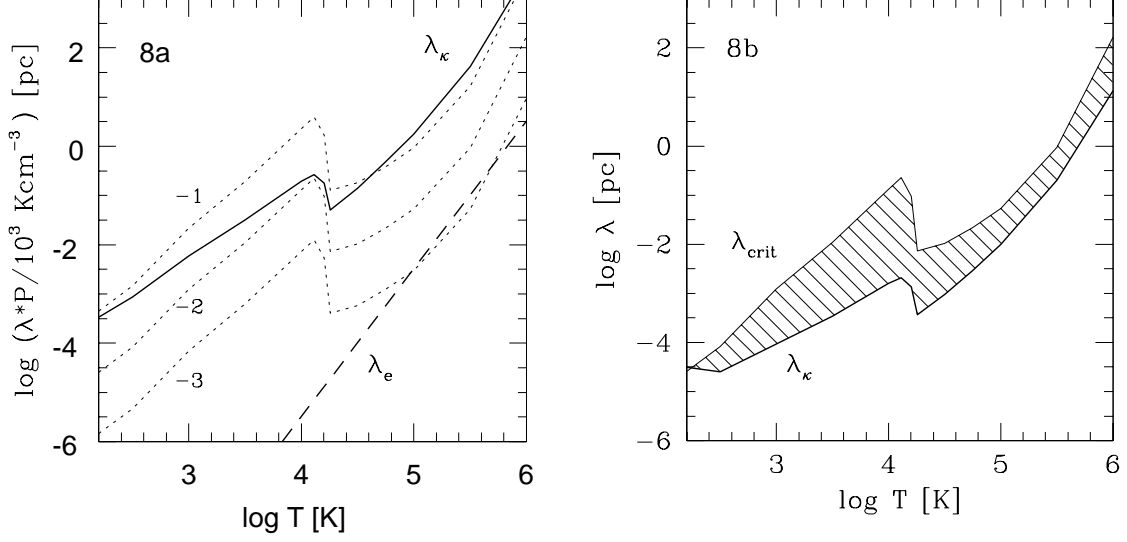


Fig. 8.— Fig. 8a shows several interesting lengthscales as function of temperature, adopting a gas pressure of  $P/k_B = nT = 10^3 \text{ K cm}^{-3}$ . Solid line:  $\lambda_\kappa$ . Dashed lines:  $\lambda_{crit}$  for density fluctuations with  $\log(\rho_a/\rho_0) = -1, -2, -3$ , respectively. Dashed line:  $\lambda_e$ . The shaded area in Fig. 8b shows the wavelength regime  $\lambda_\kappa \leq \lambda \leq \lambda_{crit}$  where density perturbations with  $\log(\rho_a/\rho_0) = -2$  would be able to grow and become non-linear, adopting a gas pressure of  $P/k_B = 10^3 \text{ K cm}^{-3}$ , a magnetic field of  $B = 0.01 B_T$  and a tangled magnetic field length scale of  $l_B = 0.1 \lambda_e$ .

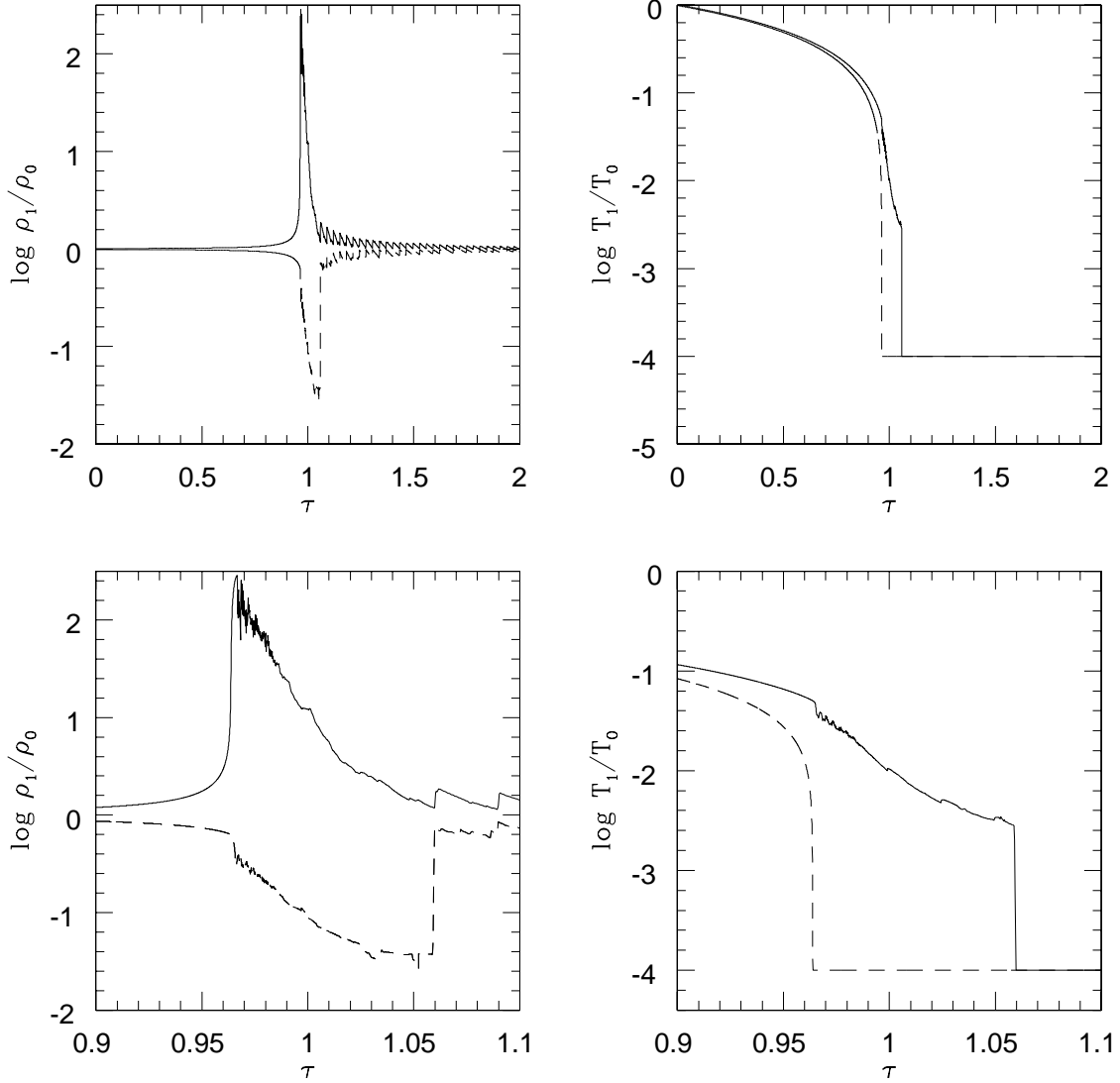


Fig. 9.— Evolution of a nonlinear perturbation with  $K=1000$  and  $\beta = 0$ . The upper panels show the evolution of the maximum density and temperature (solid line) and of the minimum density and temperature (dashed lines) for 2 cooling timescales. Shortly after one cooling timescale the low-density regions cool down to the minimum temperature too and the reversed pressure gradient erases the density contrast. The lower panels show the evolution of the density and temperature during the short epoch at  $\tau \approx 1$  when a 2-phase medium has formed.

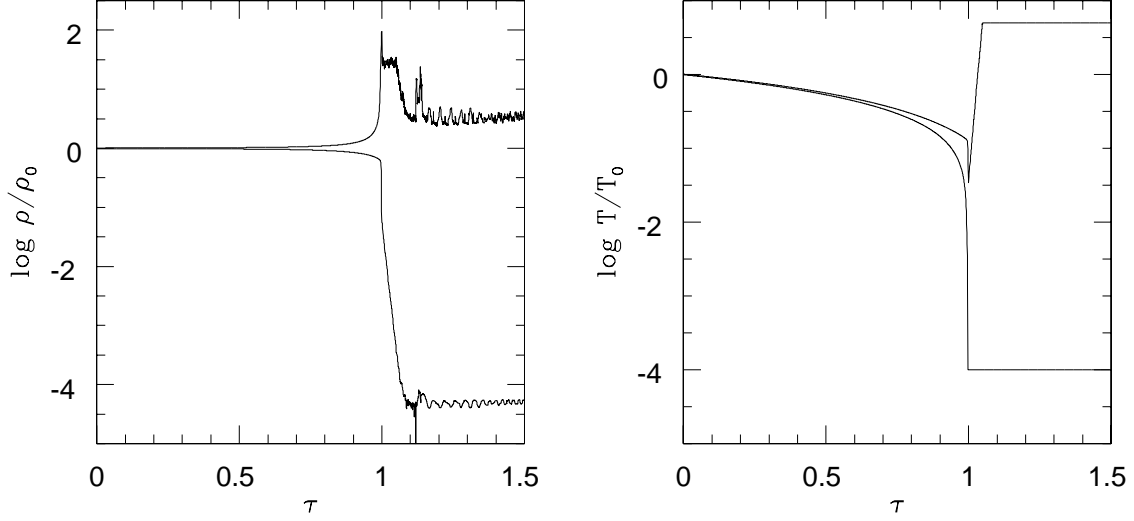


Fig. 10.— The evolution of the maximum and minimum density (left panel) and maximum and minimum temperature (right panel) of a non-linear perturbation, including a cooling term with  $\beta = 0$  and a heating term which dominates for  $\rho < \rho_\Gamma = 0.1\rho_0$ , where  $\rho_0$  is the initial average density. The density perturbation grows and becomes non-linear within a cooling timescale. As gas is pushed into the high-density regions, the density in the inter-clump region decreases below the critical value where heating begins to dominate and the inter-clump gas heats up. A stable two-phase medium forms.